# miR-150-5p Inhibits Non-Small-Cell Lung Cancer Metastasis and Recurrence by Targeting HMGA2 and β-Catenin Signaling

Fu-Qiang Dai,[1,4] Cheng-Run Li,[2,4] Xiao-Qing Fan,[1] Long Tan,[1] Ren-Tao Wang,[3] and Hua Jin[1]

[1]Department of Thoracic Surgery, Daping Hospital and Research Institute of Surgery, Third Military Medical University, Chongqing 400042, China; [2]Department of Thoracic Surgery, The General Hospital of Chinese People's Liberation Army, Beijing 100853, China; [3]Department of Respiratory, The General Hospital of Chinese People's Liberation Army, Beijing 100853, China

**Dysregulated microRNAs (miRNAs) play crucial roles in the regulation of cancer stem cells (CSCs), and CSCs are closely associated with tumor initiation, metastasis, and recurrence. Here we found that miR-150-5p was significantly downregulated in CSCs of non-small-cell lung cancer (NSCLC) and its expression level was negatively correlated with disease progression and poor survival in patients with NSCLC. Inhibition of miR-150-5p increased the CSC population and sphere formation of NSCLC cells *in vitro* and stimulated NSCLC cell tumorigenicity and metastatic colonization *in vivo*. In contrast, miR-150-5p overexpression potently inhibited sphere-formed NSCLC cell tumor formation, metastatic colonization, and recurrence in xenograft models. Furthermore, we identified that miR-150-5p significantly inhibited wingless (Wnt)-β-catenin signaling by simultaneously targeting glycogen synthase kinase 3 beta interacting protein (GSKIP) and β-catenin in NSCLC cells. miR-150-5p also targeted high mobility group AT-hook 2 (HMGA2), another regulator of CSCs, and Wnt-β-catenin signaling. The restoration of HMGA2 and β-catenin blocked miR-150-5p overexpression-induced inhibition of CSC traits in NSCLC cells. These findings suggest that miR-150-5p functions as a CSC suppressor and that overexpression of miR-150-5p may be a novel strategy to inhibit CSC-induced metastasis and recurrence in NSCLC.**

## INTRODUCTION

Lung cancer is a leading cause of cancer-related death worldwide, and non-small-cell lung cancer (NSCLC) is the predominant type of lung cancer, comprising approximately 80%–85% of lung cancers.[1] Despite advances that have been made in therapeutic technologies and strategies, the prognosis of this disease remains poor; the 5-year survival rate of NSCLC is only 15%.[2,3] The developments of chemoresistance, metastasis, and recurrence are the major obstacles to the improvement of patient survival.[4,5] Therefore, elucidation of the mechanisms underlying chemoresistance, metastasis, and recurrence is fundamental for the development of new therapeutic strategies in NSCLC.

Accumulating evidence shows that cancer stem cells (CSCs) play crucial roles in the development of chemoresistance, metastasis, and recurrence in cancers, including NSCLC.[6,7] CSCs are a small subpopulation of tumor cells with stem cell-like properties, such as self-renewal and differentiation, and they are highly resistant to chemotherapy.[8] These properties of CSCs allow them to survive chemotherapy and regenerate all of the cell types in the tumor, resulting in local or distant recurrence of the disease. Thus, CSCs are an important therapeutic target for cancer treatment. However, the regulatory mechanism of CSCs is not fully understood.

microRNAs are small noncoding RNAs that play important roles in many biological processes by negatively regulating gene expression through direct binding to the 3′ UTR of the mRNA of target genes, which leads to mRNA degradation or translational repression.[9] Aberrantly expressed microRNAs (miRNAs) have been detected in CSCs compared to non-CSCs, and studies have shown that dysregulated expression of miRNAs plays an important role in cancer cell stemness maintenance, thereby stimulating cancer metastasis, chemoresistance, and recurrence.[2] Interestingly, many miRNAs carry out opposite functions in different tissues and different stages of tumor progression by targeting different genes.[10–12] Dysregulated expression of miR-150-5p has been detected in CSCs of various cancer types, including liver cancer,[13] prostate cancer,[14] and leukemia.[15] Liu et al.[14] reported that miR-150-5p promotes CSCs in prostate cancer. However, Zhang et al.[13] showed that miR-150-5p inhibits CSCs in liver cancer, suggesting that miR-150-5p plays opposite roles in stem cells of different cancer types. Dysregulated expression of
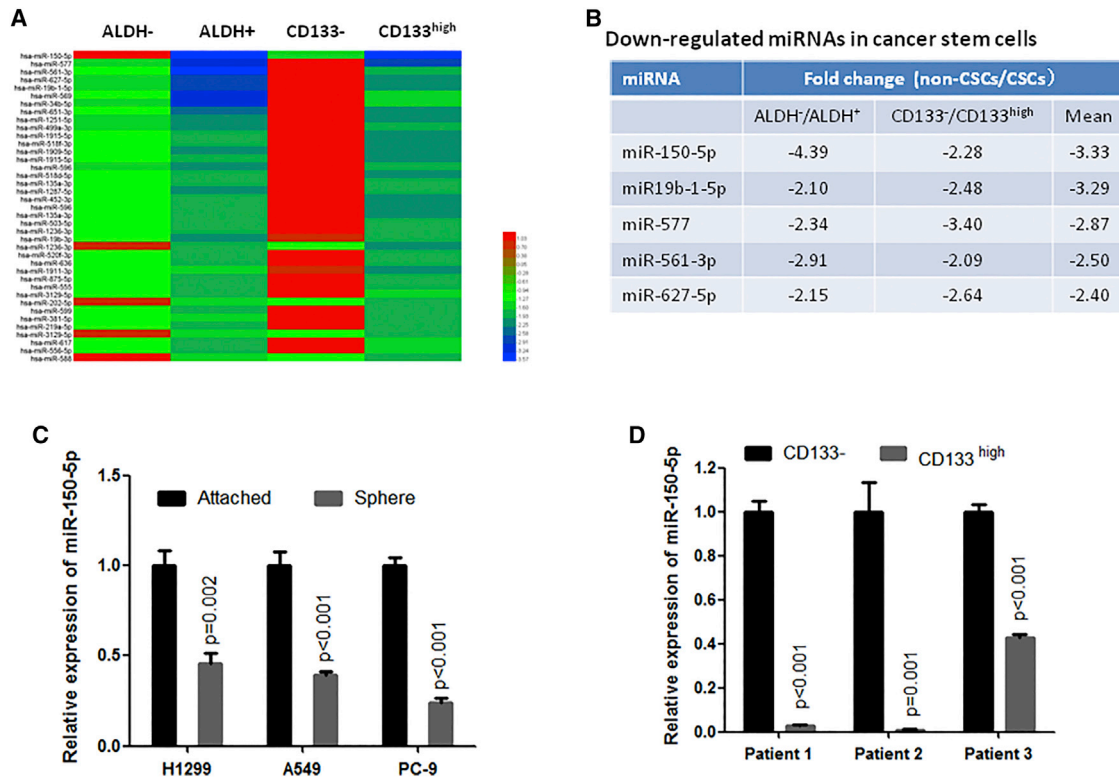
**Figure 1. miR-150-5p Was Significantly Suppressed in Cancer Stem Cells**

(A) Heatmap showing miRNAs that were downregulated by more than 1.5-fold in ALDH-positive and CD133-high-expression cells compared to ALDH-negative and CDD133-negative cells, respectively. ALDH-positive and -negative or CDD133-high-expression and -negative cells were separated from A549 cells by flow cytometry sorting and were then subjected to miRNA array assay. (B) miRNAs were simultaneously downregulated by more than 2-fold in both ALDH-positive and CD133-high-expression cells compared to ALDH-negative and CDD133-negative cells, respectively. (C) qRT-PCR analysis showed that miR-150-5p was significantly suppressed in sphere-formed NSCLC cells compared to cells that grew adherently. (D) qRT-PCR analysis showed that miR-150-5p was significantly downregulated in CD133-high-expression cells compared to CD133-negative cells from NSCLC patients (n = 3).

miR-150-5p has been detected in lung cancer;[16,17] however, miR-150-5p expression and function in lung cancer stem cells are not clear.

Here we show that miR-150-5p expression was significantly decreased in CSCs compared to non-CSCs and that decreased miR-150-5p expression was significantly associated with disease progression and poor survival in patients with NSCLC. Inhibition of miR-150-5p increased CSC population, stemness, and metastasis in NSCLC cells, while overexpression of miR-150-5p significantly inhibited tumorigenesis, recurrence, and metastasis of CSCs by targeting high mobility group AT-hook 2 (HMGA2) and β-catenin signaling in NSCLC.

## RESULTS

### miR-150-5p Is Significantly Decreased in the CSCs of NSCLC

To investigate the dysregulated miRNAs in the CSCs of NSCLC, we separated CSCs and non-CSCs from A549 cell lines using antibodies against the CSC marker proteins ALDH and CD133, and then we performed miRNA array analysis. As shown in Figure 1A, we detected a total of 39 miRNAs that were simultaneously reduced by more than 1.5-fold in both ALDH-positive and CD133-high-expression cells (CD133high) compared to ALDH-negative and CD133-negative cells (CD133−), respectively. Among them, miR-150-5p was one of the most downregulated miRNAs in CSCs compared to non-CSCs (Figure 1B).

Furthermore, we checked the miR-150-5p expression level in sphere-formed cells, because sphere-forming cells present stem cell-like properties. Consistent with the miRNA array results, we observed a significantly decreased expression of miR-150-5p in sphere-formed cells of several NSCLC cell lines compared to their control cells that grew adherently (Figure 1C). These *in vitro* results were confirmed in clinical samples. Our data show that miR-150-5p expression was significantly decreased in CD133high NSCLC cells compared to CD133-negative cells from NSCLC patients (Figure 1D). Taken together, these data suggest that decreased expression of miR-150-5p is closely involved in the regulation of CSCs in NSCLC.
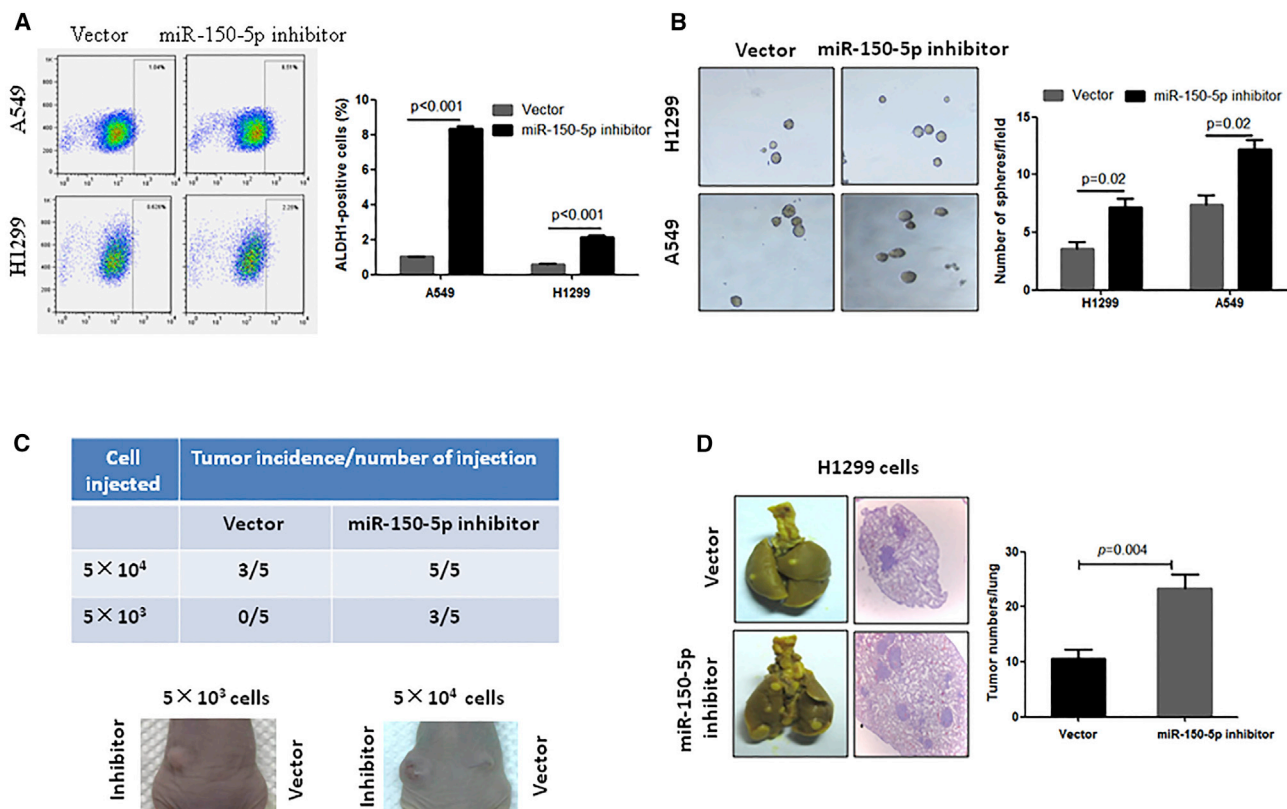
**Figure 2. Inhibition of miR-150-5p Enhanced NSCLC Cell Stemness and Metastatic Colonization**

(A) Inhibition of miR-150-5p significantly decreased ALDH-positive cells in NSCLC cells. The indicated cells were infected with miR-150-5p antisense-expressing lentivirus. At 72 h after infection, the cells were subjected to flow cytometry. (B) Inhibition of miR-150-5p significantly enhanced sphere formation in NSCLC cells. (C) Inhibition of miR-150-5p enhanced the tumorigenicity of A549 cells. A total of $5 \times 10^3$ or $5 \times 10^4$ miR-150-5p antisense-expressing A549 cells (left back) and vector control cells (right back) was subcutaneously injected into nude mice (n = 5). (D) Inhibition of miR-150-5p stimulated H1299 cell metastatic colony formation in lungs. miR-150-5p antisense-expressing A549 cells or control cells were injected into nude mice through the tail vein (n = 5). At 1 month after cell injection, mice were sacrificed and tumor colony numbers were counted on the lung surface. The histological section was stained with H&E.

## Inhibition of miR-150-5p Contributes to Stemness Maintenance and Metastatic Colonization

To investigate whether decreased expression of miR-150-5p contributes to CSC regulation and stemness maintenance, we used miR-150-5p-inhibited NSCLC cell lines (Figure S1A) to check the CSC population, sphere-forming ability, *in vivo* tumor formation ability, and metastasis. Our data show that inhibition of miR-150-5p significantly increased the aldehyde dehydrogenase 1 (ALDH1)-positive cell population (Figure 2B) and stimulated sphere formation in both H1299 and A549 NSCLC cell lines compared to their control cells (Figure 2B). In addition, the results from an *in vivo* experiment showed that subcutaneous injection of $5 \times 10^4$ A549 cells into each mouse resulted in tumor formation in 60% of mice within 2 months, but injection of miR-150-5p-inhibited A549 cells resulted in tumor formation in 100% of mice (Figure 2C). Notably, only miR-150-5p-inhibited A549 cells formed visible tumors when $5 \times 10^3$ cells were implanted (Figure 2C), indicating that the inhibition of miR-150-5p might expand the CSC population in NSCLC cells. Furthermore, we

investigated the effects of miR-150-5p inhibition on metastatic colonization because CSCs play a crucial role in the initiation of metastatic growth.[18] As shown in Figure 2D, the inhibition of miR-150-5p significantly stimulated H1299 cell colonization in the lungs compared to the vector control, suggesting that the downregulation of miR-150-5p significantly stimulates NSCLC stemness.

## Ectopic Expression of miR-150-5p Significantly Inhibits CSC-Induced Tumorigenesis, Recurrence, and Metastatic Colonization in NSCLC

Our observations that the inhibition of miR-150-5p significantly contributed to NSCLC cell stemness prompted us to investigate whether miR-150-5p overexpression could suppress CSCs in NSCLC. Because sphere-formed NSCLC cells are enriched with CSCs,[19] the sphere-formed A549 or H1299 cells were infected with miR-150-5p-expressing lentivirus (Figure S1B), and they were then subjected to an *in vitro* sphere formation assay and *in vivo* tumor formation.
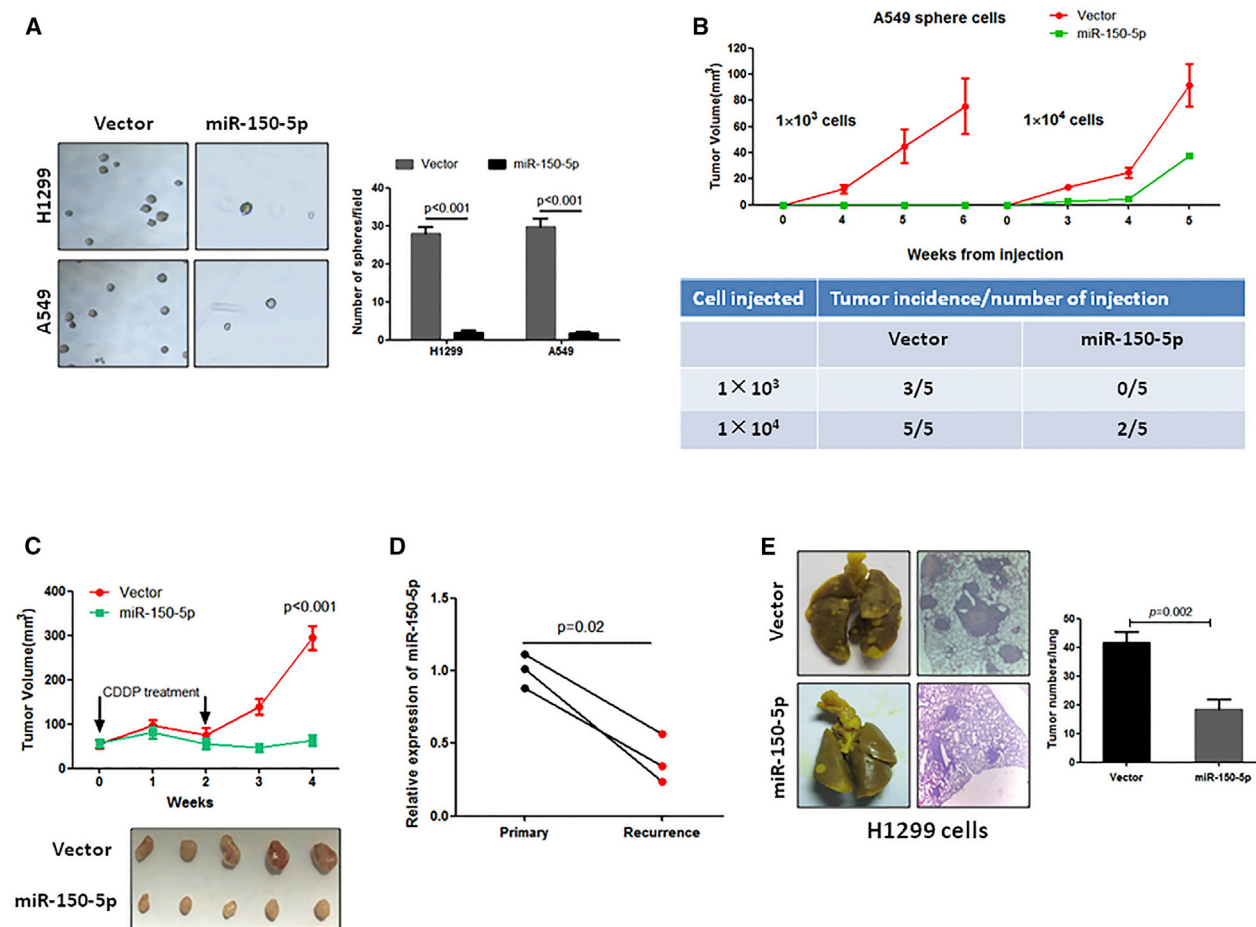
**Figure 3. Overexpression of miR-150-5p Inhibited Sphere-Formed NSCLC Cell-Induced Tumorigenesis, Recurrence, and Metastasis**

(A) Overexpression of miR-150-5p significantly inhibited sphere formation in sphere-formed NSCLC cells. The indicated cells were subjected to sphere formation. After 1 week of incubation, spheres were harvested and infected with miR-150-5p-expressing lentivirus. At 12 h after infection, cells were subjected to second-round sphere formation. (B) Overexpression of miR-150-5p dramatically inhibited tumor formation of sphere-formed A549 cells in nude mice (n = 5). Sphere-formed A549 cells were infected with miR-150-5p-expressing lentivirus or an empty vector, and they were then subcutaneously injected into nude mice at an indicated dose. (C) Overexpression of miR-150-5p prevented NSCLC relapse. Sphere-formed A549 cells were infected with miR-150-5p-expressing lentivirus or an empty vector, and they were then subcutaneously injected into nude mice (n = 5). When the mean tumor volume reached 50 $mm^3$, the mice were treated with CDDP for 2 weeks, and the tumor volumes were measured 2 weeks after the end of CDDP treatment. (D) qRT-PCR analysis showed that miR-150-5p expression was significantly decreased in recurrent NSCLC specimens compared to their corresponding primary tumors (n = 3). (E) Overexpression of miR-150-5p inhibited metastatic colony formation of sphere-formed H1299 cells. Sphere-formed H1299 cells were infected with miR-150-5p-expressing lentivirus or an empty vector and they were then injected into nude mice through the tail vein (n = 5). At 1 month after cell injection, the mice were sacrificed and the tumor numbers on the lung surface were counted. The histological section was stained with H&E.

As shown in Figure 3A, the overexpression of miR-150-5p dramatically inhibited sphere formation in both sphere-forming H1299 and A549 cells. In addition, *in vivo* tumor formation experiments showed that tumors were formed in 100% of mice in the vector control group, while only 40% of mice formed tumors in the miR-150-5p-overexpressing group when each mouse was subcutaneously injected with $1 \times 10^4$ sphere-forming A549 cells (Figure 3B). Notably, implantation with $1 \times 10^3$ sphere-forming A549 cells induced tumor formation in 60% of nude mice, but implantation with miR-150-5p-overexpressing A549 sphere-forming cells did not induce tumor formation when each mouse was injected with $1 \times 10^3$ cells (Figure 3B). *In vivo* tumor

formation experiments also showed that the overexpression of miR-150-5p significantly delayed tumor-forming time in A549 sphere-forming cells (Figure 3B).

Because CSCs play a crucial role in cancer relapse, we investigated the effects of miR-150-5p on CSC-induced NSCLC relapse. When the mean tumor volume reached ∼50 $mm^3$, mice inoculated with sphere-formed A549 cells or miR-150-5p-overexpressing sphere-formed A549 cells began to receive cisplatin (CDDP) treatment. As shown in Figure 3C, CDDP treatment transiently reduced tumor volume but relapse of the disease occurred in the control group after
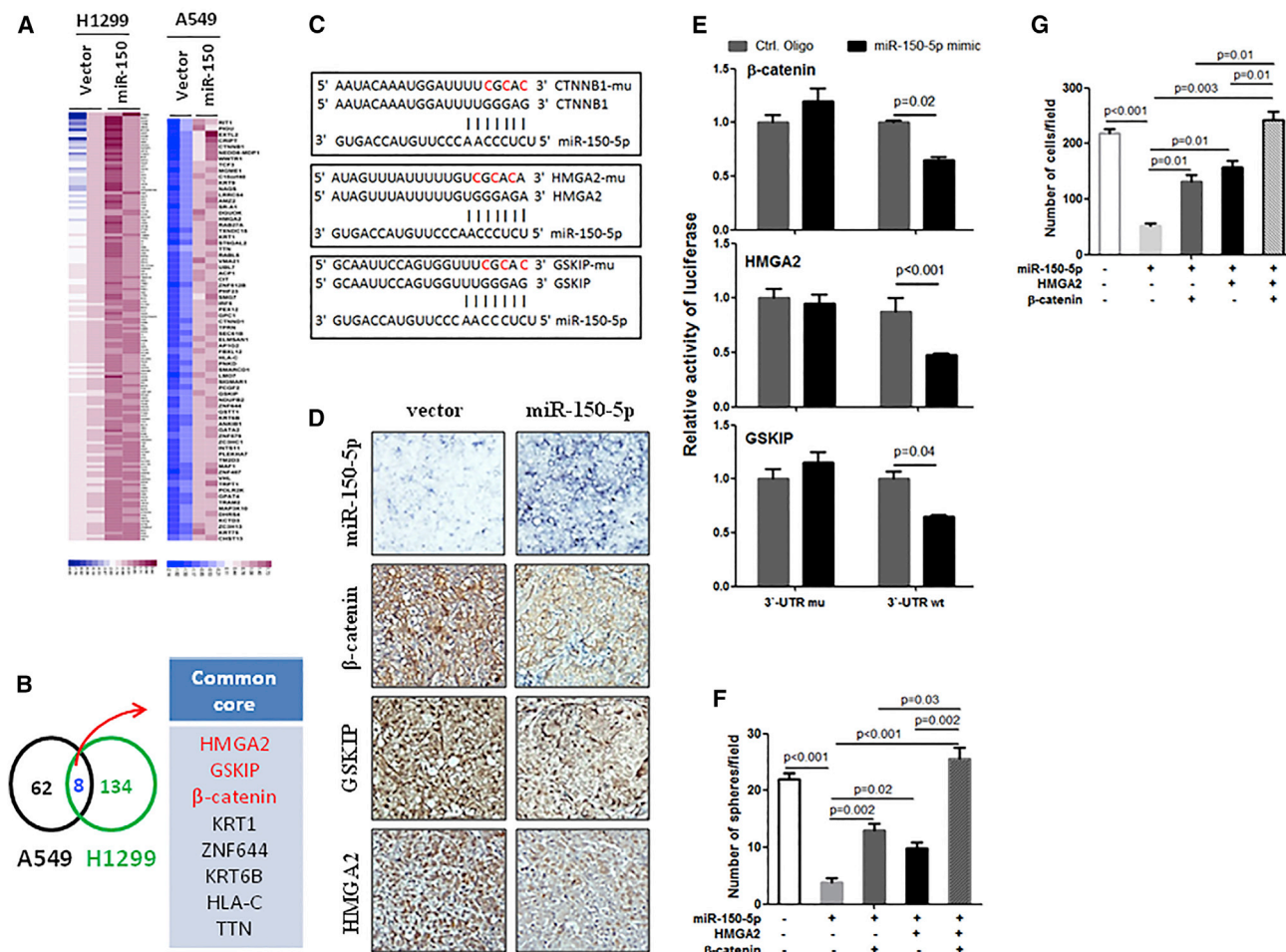
**Figure 4. miR-150-5p Targeting HMGA2 and Wnt-β-Catenin Signaling in NSCLC**

(A) Heatmap showing proteins that were downregulated by miR-150-5p by more than 1.5-fold in sphere-formed NSCLC cells. Sphere-formed H1299 or A549 cells were infected with miR-150-5p-expressing lentivirus or an empty vector. After 48 h, the cells were subjected to proteomics analysis. (B) Venn diagram showing substantial overlap of core proteins from H1299 and A549 cell lines. (C) Predicted binding sites of miR-150-5p in the wild-type 3′ UTRs of HMGA2, GSKIP, and β-catenin (CTNNB1). Mutations in these 3′ UTRs are highlighted in red. (D) HMGA2, GSKIP, and β-catenin expressions were significantly downregulated by miR-150-5p. The expression levels of the indicated proteins were measured using immunohistochemistry (IHC). Tissues from the lung metastasis model were generated with sphere-formed H1299 cells that were infected with miR-150-5p-expressing lentivirus or an empty vector. (E) Luciferase activity of reporter with wild-type or mutant 3′ UTRs of HMGA2, GSKIP, and β-catenin in the A549 cells cotransfected with control oligonucleotides or miR-150-5p mimics. (F) Restored HMGA2 and/or β-catenin blocked miR-150-5p-induced inhibition of sphere formation in sphere-formed H1299 cells. Sphere-formed H1299 cells were infected with the indicated gene expression lentivirus for 24 h, and they were then subjected to sphere formation. (G) Restored HMGA2 and/or β-catenin blocked the inhibition of invasion by miR-150-5p in sphere-formed H1299 cells. Sphere-formed H1299 cells were infected with the indicated gene expression lentivirus for 24 h, and they were then subjected to an invasion assay.

stopping the CDDP treatment. In contrast, tumors expressing a higher level of miR-150-5p failed to regrow after CDDP treatment ended, suggesting that miR-150-5p negatively regulates NSCLC recurrence. Notably, we detected an inverse correlation between miR-150-5p expression level and recurrence of NSCLC (Figure 3D).

Furthermore, we investigated the effects of miR-150-5p on CSC-induced metastatic colonization. Our data show that the overexpression of miR-150-5p dramatically suppressed sphere-forming H1299 cell-induced metastatic colonization in the lungs (Figure 3E). Taken

together, our findings suggest that miR-150-5p can inhibit CSC-induced tumorigenesis, recurrence, and metastasis in NSCLC.

## miR-150-5p Simultaneously Targets HMGA2, GSKIP, and β-Catenin

To investigate the underlying mechanism of the effects of miR-150-5p on the regulation of NSCLC stemness, we identified proteins that were downregulated by miR-150-5p overexpression in sphere-formed NSCLC cells. As shown in Figure 4A, we observed global changes in protein expression in miR-150-5p-overexpressing sphere-formed

**Table 1. Characteristics of Patients with NSCLC**

| Variable | Number of Patients (%) | | |
|---|---|---|---|
| | miR150 Low (n = 47) | miR150 High (n = 64) | p |
| Gender | | | |
|   Male | 35 (74.47) | 49 (76.56) | 0.80 |
|   Female | 12 (25.53) | 15 (23.44) | |
| Age | | | |
|   ≤60 | 27 (57.45) | 35 (54.69) | 0.77 |
|   >60 | 20 (42.55) | 29 (45.31) | |
| Smoking | | | |
|   Yes | 27 (57.45) | 41 (64.06) | 0.48 |
|   No | 20 (42.55) | 23 (35.94) | |
| Histology | | | |
|   Adenocarcinoma | 23 (48.94) | 29 (45.31) | |
|   Squamous cell carcinoma | 22 (46.80) | 29 (45.31) | |
|   Bronchioloalveolar carcinoma | 0 (0.00) | 1 (1.56) | 0.48 |
|   Large-cell carcinoma | 0 (0.00) | 2 (3.13) | |
|   Carcinoid | 0 (0.00) | 2 (3.13) | |
|   Other | 2 (4.26) | 1 (1.56) | |
| T status | | | |
|   T1 | 7 (14.89) | 12 (18.75) | |
|   T2 | 22 (46.81) | 34 (53.12) | 0.49 |
|   T3 | 13 (27.66) | 10 (15.63) | |
|   T4 | 5 (10.64) | 8 (12.50) | |
| N status | | | |
|   N0 | 20 (42.55) | 48 (75.00) | |
|   N1 | 15 (29.79) | 9 (15.63) | 0.01 |
|   N2 | 11 (25.53) | 7 (9.37) | |
|   N3 | 1 (2.13) | 0 (0.00) | |
| M status | | | |
|   M0 | 44 (87.23) | 64 (95.31) | 0.04 |
|   M1 | 3 (2.13) | 0 (0.00) | |

A549 and H1299 cells compared to their corresponding control cells (Figure 4A). However, we observed only 8 proteins whose gene 3′ UTRs contained miR-150-5p-binding sequences, which were simultaneously downregulated in both A549 and H1299 cells compared to their control cells (Figure 4B). Among them, we selected HMGA2, glycogen synthase kinase 3 beta interacting protein (GSKIP), and β-catenin as candidate target genes of miR-150-5p (Figure 4C).

Wingless (Wnt)-β-catenin signaling plays a crucial role in cancer cell stemness maintenance, and GSKIP and β-catenin are involved in Wnt-β-catenin-signaling activation.[20,21] Additionally, studies have shown that HMGA2 promotes cancer cell stemness and β-catenin signaling.[22,23] To investigate whether miR-150-5p inhibits the expres-

sion of these genes, we measured the expression levels of miR-150-5p and its target genes in tumor tissues from a xenograft model generated by miR-150-5p-overexpressing spheres that formed H1299 cells and control cells. Our data show that expressions of HMGA2, GSKIP, and β-catenin were significantly decreased in miR-150-5p high-expressing tumors compared to miR-150-5p low-expressing tumors (Figure 4D). Next, we investigated whether the regulation of HMGA-, GSKIP-, and β-catenin-luciferase expressions depends on the binding of their complementary 3′ UTR sequences to the miR-150-5p seed sequence. A 3-nt mutation was inserted into the HMGA, GSKIP, and β-catenin 3′ UTRs, as indicated in Figure 4C. Ectopic expression of miR-150-5p significantly repressed luciferase activity in the wild-type 3′ UTR setting. In contrast, 3′ UTR mutations completely abrogated the effect of miR-150-5p overexpression on luciferase activity (Figure 4E). Cumulatively, these data suggest that miR-150-5p negatively regulates the expressions of HMGA2, GSKIP, and β-catenin by directly targeting their 3′ UTR sequences in the CSCs of NSCLC.

Furthermore, we investigated whether HMGA2 and β-catenin signaling is directly involved in miR-150-5p function. HMGA2 and β-catenin were overexpressed in miR-150-5p-overexpressing spheres that formed H1299 cells, and the cells were subjected to sphere and invasion assays. Our results show that exogenously expressed HMGA2 or β-catenin partially blocked miR-150-5p-induced inhibition of sphere formation (Figure 4F; Figure S2A) and invasion (Figure 4G; Figure S2B). Interestingly, simultaneous expression of HMGA2 and β-catenin more completely blocked miR-150-5p-induced inhibition of sphere formation and invasion than single overexpression of HMGA2 or β-catenin (Figures 4F and 4G; Figure S2), suggesting that miR-150-5p plays an anti-CSC role through HMGA2 and β-catenin in NSCLC.

### Clinical Relevance of miR-150-5p and Its Target Genes in NSCLC

Finally, we examined whether miR-150-5p and its target gene expressions were clinically relevant in NSCLC. A total of 111 patients with NSCLC was divided into miR-150-5p high- and low-expression groups based on miR-150-5p *in situ* hybridization (ISH) results (Figure S3; Table 1). Clinical data show that the miR-150-5p expression level was negatively correlated with metastasis, including lymph node and distant metastasis, at the time of diagnosis in NSCLC patients (Table 1). Notably, follow-up data show that the relapse rates of NSCLC patients with lower and higher miR-150-5p expressions were 51% and 25% (Figure 5A), respectively, and the median times to progression for the miR-150-5p low- and high-expression cases were 28 months and 56.5 months, respectively (Figure 5C). Consistent with these data, the NSCLC patient group with low expression of miR-150-5p had a poor progression-free survival rate (Figure 5B) and a poor overall survival rate compared to the miR-150-5p high-expression group (Figure 5C). Consistent with our clinical data, The Cancer Genome Atlas (TCGA) dataset analysis also showed that the expression level of miR-150-5p was negatively correlated with overall survival in NSCLC patients (Figure 5D). Taken together, these data suggest
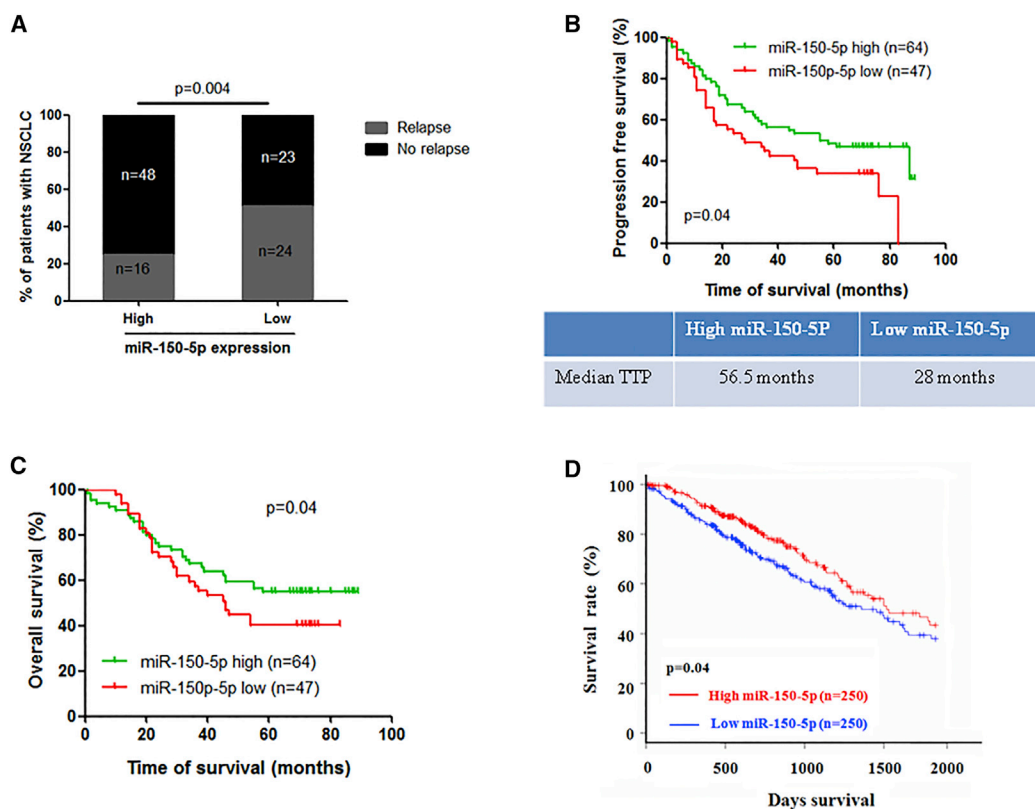
**Figure 5. Clinical Relevance of miR-150-5p Expression in NSCLC Patients**

(A) The miR-150-5p expression level was negatively correlated with recurrence in NSCLC patients. (B) NSCLC patients in the miR-150-5p low-expression group had a significantly lower progression-free survival rate and shorter median time to progression (TTP) than those in the miR-150-5p high-expression group. (C) NSCLC patients in the miR-150-5p low-expression group had a significantly lower overall survival rate than those in the miR-150-5p high-expression group. (D) TCGA (The Cancer Genome Atlas) dataset analysis showed that lung adenocarcinoma patients in the miR-150-5p low-expression group had a significantly lower overall survival rate than those in the miR-150-5p high-expression group.

that decreased expression of miR-150-5p is closely correlated with disease progression in patients with NSCLC.

Additionally, we examined the correlation of miR-150-5p and its target gene expressions in NSCLC specimens. As shown in Figures 6A and 6B, correlation studies in the aforementioned 111 NSCLC specimens showed an inverse correlation between the expression levels of miR-150-5p and those of its targets. Specifically, 62% (29 cases), 62% (29 cases), and 57% (27 cases) of cases with low miR-150-5p expression (47 cases) showed high expressions of HMGA2, GSKIP, and β-catenin, respectively, whereas 72% (46 cases), 78% (50 cases), and 72% (46 cases) of specimens with high miR-150-5p expression (64 cases) exhibited low levels of HMGA2, GSKIP, and β-catenin, respectively (Figure 6B). In addition, the data show that high expressions of miR-150-5p target genes were associated with poor clinical outcomes in NSCLC patients (Figure 6C). These data suggest that HMGA2, GSKIP, and β-catenin are major target genes of miR-150-5p in NSCLC and that miR-150-5p and its target gene expressions may be a useful prognostic signature of NSCLC.

## DISCUSSION

The occurrence of metastasis or relapse in cancer patients indicates poor prognosis. Thus, the identification of prognostic factors that can stratify patients according to clinical and biological markers may help to select adequate treatment strategies.[24] Unfortunately, there are no biomarkers to predict NSCLC progression. Here, our clinical data show that the NSCLC patient group with a low expression level of miR-150-5p had a shorter median time to progression, progression-free time, and overall survival time and a higher relapse rate, suggesting that miR-150-5p has potential as a biomarker for predicting NSCLC progression. These data need to be further studied in a larger sample scale to demonstrate the prognostic value of miR-150-5p expression as a clinically useful independent indicator of NSCLC patient outcome assessment.

CSCs play key roles in cancer progression, including metastasis and recurrence. Thus, CSCs are important targets for cancer treatment. In this study, we demonstrated significantly decreased expression of miR-150-5p in the CSCs of NSCLC and recurrent NSCLC samples compared to non-CSCs and their primary tumors, respectively. These
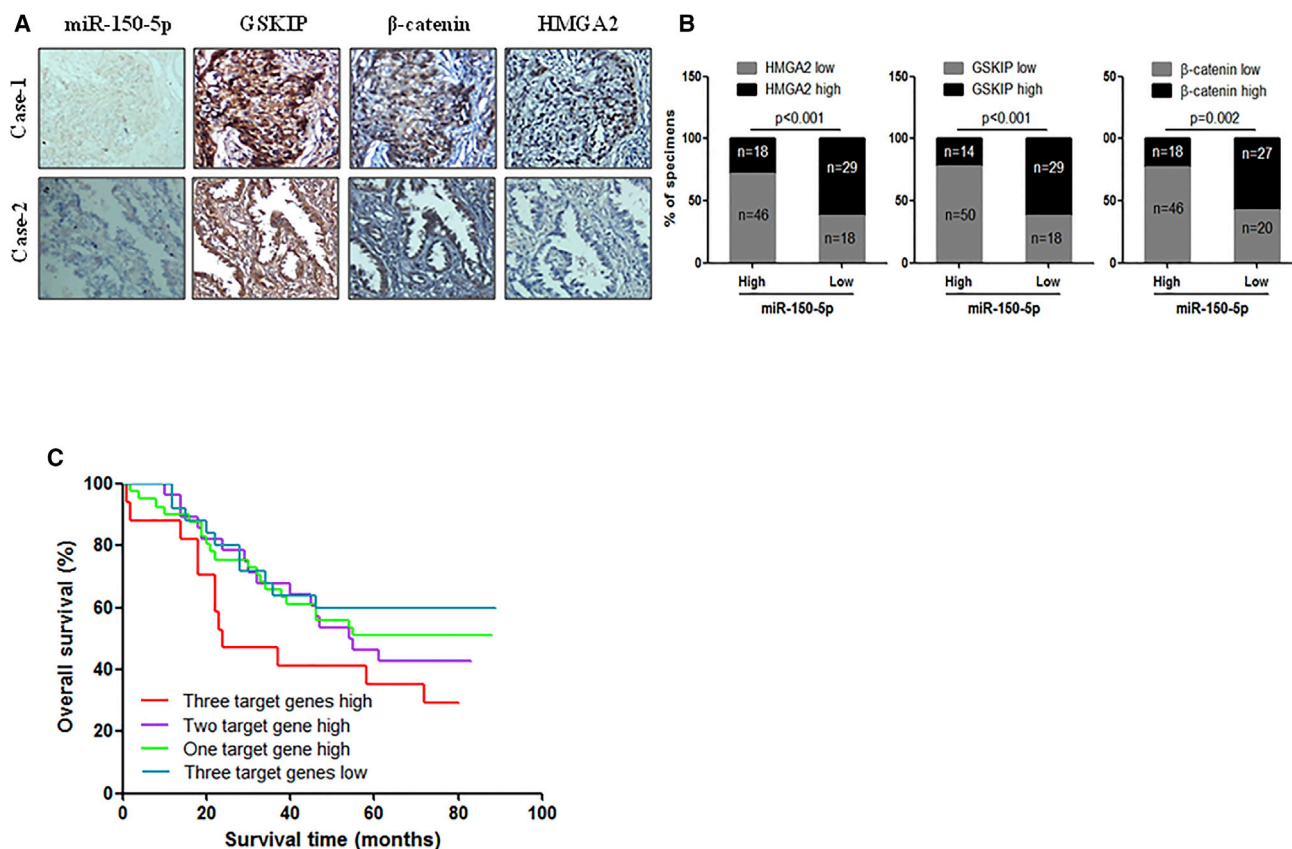
**Figure 6. Correlation of miR-150-5p and Its Target Gene Expressions in NSCLC Specimens**

(A) ISH of miR150-5p and IHC analysis of HMGA2, GSKIP, and β-catenin in serial sections of NSCLC tumor specimens. (B) The correlation between miR-150-5p and its target genes in NSCLC specimens. (C) The correlation between HMGA2 and β-catenin levels and overall survival rate in 111 NSCLC patients was analyzed using the Kaplan-Meier method.

findings suggest that miR-150-5p may be negatively involved in CSC regulation, thereby affecting CSC-induced relapse and metastasis. Indeed, our *in vitro* and *in vivo* experiment results show that the inhibition of miR-150-5p stimulates NSCLC cell sphere formation, tumorigenic ability, and metastatic colonization, whereas the overexpression of miR-150-5p dramatically inhibits CSC-induced tumorigenesis, recurrence, and metastatic colonization of NSCLC cells. Consistent with our findings, previous studies have shown that miR-150-5p was significantly downregulated in the CSCs of liver cancer[13] and leukemia[15] and negatively regulated cancer stemness. These findings also suggest that the overexpression of miR-150-5p may be a strategy to treat CSCs that cause relapse and metastasis.

In this study, we also clarified the CSC inhibition mechanisms of miR-150-5p in NSCLC. Evidence indicates that constitutively activated Wnt-β-catenin signaling[2,25] and upregulated HMGA2[22,26,27] are critical for the development and maintenance of CSCs and are closely associated with cancer progression, including metastasis and recurrence. Here we identified GSKIP, β-catenin, and HMGA2 as targets of miR-150-5p in NSCLC. Consistent with our findings, previous

studies have identified β-catenin[28] and HMGA2[23] as targets of miR-150-5p in leukemia stem cells[15] and breast cancer,[29] respectively. β-catenin is a well-studied activator of Wnt-β-catenin that is closely associated with NSCLC progression.[28] GSKIP is an activator of Wnt-β-catenin signaling that causes β-catenin upregulation by negatively regulating the β-catenin inhibitor GSK3β.[30,31] HMGA2 is a transcription-regulating factor that plays an oncogenic role through Wnt-β-catenin signaling and independently.[32–34] Our data show that ectopic expression of HMGA2 and activation of β-catenin signaling can completely block miR-150-5p-induced CSC inhibition effects in NSCLC. Notably, our clinical data show that miR-150-5p expression is negatively correlated with GSKIP, β-catenin, and HMGA2 expressions in NSCLC specimens and these target gene expressions also correlated with the overall survival of NSCLC patients, suggesting that miR-150-5p plays an anticancer role by targeting HMGA2 and Wnt-β-catenin signaling in NSCLC.

In summary, we combined clinical and experimental studies to determine the clinical significance and the roles of miR-150-5p in NSCLC. Our findings suggest that aberrantly downregulated expression of

miR-150-5p in the CSCs of NSCLC contributes to cancer stemness maintenance, metastasis, and recurrence. The overexpression of miR-150-5p suppressed CSC-induced tumorigenesis, recurrence, and metastasis in NSCLC, suggesting that our findings may also aid in the development of potential therapeutics for the treatment of CSC-induced progression of NSCLC.

## MATERIALS AND METHODS

### Materials
Fetal bovine serum (FBS), cell culture medium, penicillin-streptomycin solution, cisplatin, hydrocortisone, basic fibroblast growth factor (bFGF), and insulin were purchased from Sigma-Aldrich (St. Louis, MO, USA). Lentivirus systems for expressing miR-150-5p, miR-150-5p inhibitor, GSKIP, HMGA2, and β-catenin were obtained from Genechem (Shanghai, China). Antibodies against HMGA2, β-catenin, and actin were purchased from Cell Signaling Technology (Danvers, MA, USA). CD133 antibody and the AldeFluor fluorescent system were purchased from Abcam (Cambridge, MA, USA) and STEMCELL Technologies (Vancouver, BC, Canada), respectively. The pMIR-REPORT luciferase vector and Dual-Luciferase Reporter Assay System were purchased from Ambion (Cambridge, MA, USA) and Promega (Madison, WI, USA), respectively. The 24-well ultra-low attachment plates and cell invasion assay chambers were purchased from Corning (NY, USA). The DIG system for the detection of nucleic acids was purchased from Roche (Mannelm, Germany). TRIzol reagent was obtained from Life Technologies.

### Cell Culture and Specimens
NSCLC cell lines were obtained from the American Type Culture Collection (Rockville, MD, USA) and cultured in RPMI-1640 medium supplemented with 10% FBS.

Human specimens were obtained during surgery under a protocol approved by the Daping Hospital and Research Institute of Surgery review boards. NSCLC patients were divided into miR-150-5p high and low groups, as described previously.[35] Briefly, mature miR-150-5p and the RNU6 endogenous control were analyzed using the TaqMan microRNA Assay Kit. The relative expression of miR-150-5p was normalized against RNU6 expression using the $2^{-\Delta Ct}$ method, and the miR-150-5p expression fold change in lung cancer samples matched to nontumor control samples was evaluated using the $2^{-\Delta Ct}$ method. On the basis of the mean fold change of miR-150-5p expression, patients were divided into miR-150-5p high- (fold change > mean) and low- (fold change < mean) expression groups. The demographic information of the cohort is presented in Table 1.

### Invasion and Sphere Formation Assays
For the invasion assay, $1 \times 10^5$ cells in serum-free growth medium were seeded in the upper wells of invasion chambers (12-well plate). The lower wells contained the same medium with 10% serum. After 24 h, the cells that had migrated to the lower side of the chamber were fixed with 2.5% glutaraldehyde, stained with 0.1% crystal violet, and counted.

Sphere assays were performed as described previously.[36,37] Briefly, cells were grown in DMEM-F12, supplemented with 20 ng/mL epidermal growth factor (EGF) and bFGF and 4 μg/mL insulin, and plated at 1,000 cells/mL in ultra-low adherent 24-well plates. EGF, bFGF (20 ng/mL), and insulin (4 μg/mL) were added every 3 days.

### Immunoblotting and ISH
Western blotting and immunohistochemistry were performed as described previously.[38] For in situ detection of miR-150-5p, locked nucleic acid probes were synthesized complementarily to human mature miR-150-5p (digoxigenin labeled at the 5′ end), and ISH was performed using paraffin-embedded, formalin-fixed tissues as described by Nuovo.[39]

### Luciferase Reporter Assay
The 3′ UTR segments of GSKIP, β-catenin, and HMGA2 that were predicted to interact with miR-150-5p were amplified by PCR from human genomic DNA, and they were inserted into the *Mlu I* and *Hind III* sites of the miRNA Expression Reporter Vector. For the luciferase reporter experiments, cells were seeded into 24-well cell culture plates at a concentration of $1 \times 10^4$ cells/well. The next day, the cells were transfected with the indicated reporter plasmids containing firefly luciferase and either the miR-150-5p mimics or control oligonucleotides. The Renilla luciferase plasmid was cotransfected as a transfection control. Cells were lysed 48 h after transfection, and luciferase activity was measured by the Dual-Luciferase Assay System, according to the manufacturer's protocol. The luciferase activity was normalized to the activity of Renilla luciferase.

### Flow Cytometric Analysis
CSCs were detected by flow cytometric analysis using antibodies of CD133 and ALDH1.[40] ALDH1-positive cells were detected or isolated using the AldeFluor fluorescent reagent system, according to the manufacturer's instructions. CD133-high-expression cells were detected or isolated using a CD133 antibody, according to the manufacturer's instructions.

### miRNA Array and Proteomics Analysis
Total RNA was isolated using TRIzol reagent and subjected to miRNA array analysis. The miRNA array was performed using miR-CURY LNA Array micrRNA Array 7th Gen (Exiqon), as described by Othumpangat et al.[41]

For the detection of proteins reduced by miR-150-5p, sphere-formed A549 and miR-1299 cells were infected with miR-150-5p-expressing lentivirus or an empty vector. After 48 h of transfection, proteins were extracted from cells and denatured according to the filter-aided sample prep (FASP) procedure. Then, 100 mg lysate proteins were digested with trypsin and the tryptic peptide was labeled with iTRAQ reagent. The labeled peptides were fractionated using an Agilent 1260 infinity II HPLC system and fractions were dried in a vacuum concentrator. Mass spectrometry data were collected on a Q-Exactive plus mass spectrometer (Thermo Fisher Scientific) coupled with an

Easy-nLC system (Thermo Fisher Scientific). The data were analyzed using Mascot 2.6 and Proteome Discoverer 2.1.

**Animal Experiments**

To investigate the effects of miR-150-5p inhibition on NSCLC cell tumorigenicity and metastasis, the indicated cells were infected with miR-150-5p antisense-expressing lentivirus. After 72 h of infection, cells in 100 μL PBS were injected into the subcutaneous or tail vein. Experiments were conducted for 2 months.

To investigate the effects of miR-150-5p overexpression on CSC tumorigenesis, metastatic colony formation, and relapse, the indicated sphere-formed cells were infected with miR-150-5p-expressing lentivirus. After 12 h of infection, cells in 100 μL PBS were injected into the subcutaneous or tail vein. Tumor formation and lung metastasis experiments were conducted for 6 weeks and 1 month, respectively. For the relapse experiment, when the mean tumor size reached 50 mm$^3$, the mice were treated with cisplatin (5 mg/kg body weight) every 2 days. Cisplatin treatment occurred over 2 weeks, and tumor growth was measured 2 weeks after the end of cisplatin treatment.

**Statistical Analysis**

The survival rate was calculated using the Kaplan-Meier method. The $\chi^2$ test was used to analyze the relationship between the expression levels of miR-150-5p and target genes. Differences between groups were determined by unpaired Student's t test or one-way ANOVA using the SAS statistical software package version 6.12 (SAS Institute). A p value < 0.05 was considered statistically significant.

## SUPPLEMENTAL INFORMATION

Supplemental Information can be found online at https://doi.org/10.1016/j.omtn.2019.04.017.

## AUTHOR CONTRIBUTIONS

H.J. and R.-T.W. contributed to the conception and design of the study. F.-Q.D., R.-T.W., and C.-R.L. collected the human samples and performed IHC. F.-Q.D., C.-R.L., X.-Q.F., and L.T. performed laboratory and animal experiments. H.J., R.-T.W., F.-Q.D., and C.-R.L. analyzed the data. H.J. wrote the manuscript.

## CONFLICTS OF INTEREST

The authors declare no competing interests.

## ACKNOWLEDGMENTS

## REFERENCES

1. Goldstraw, P., Ball, D., Jett, J.R., Le Chevalier, T., Lim, E., Nicholson, A.G., and Shepherd, F.A. (2011). Non-small-cell lung cancer. Lancet *378*, 1727–1740.

2. Fang, L., Cai, J., Chen, B., Wu, S., Li, R., Xu, X., Yang, Y., Guan, H., Zhu, X., Zhang, L., et al. (2015). Aberrantly expressed miR-582-3p maintains lung cancer stem cell-like traits by activating Wnt/β-catenin signalling. Nat. Commun. *6*, 8640.

3. Siegel, R., Naishadham, D., and Jemal, A. (2013). Cancer statistics, 2013. CA Cancer J. Clin. *63*, 11–30.

4. Taylor, M.D., Nagji, A.S., Bhamidipati, C.M., Theodosakis, N., Kozower, B.D., Lau, C.L., and Jones, D.R. (2012). Tumor recurrence after complete resection for non-small cell lung cancer. Ann. Thorac. Surg. *93*, 1813–1820, discussion 1820–1821.

5. Chang, A. (2011). Chemotherapy, chemoresistance and the changing treatment landscape for NSCLC. Lung Cancer *71*, 3–10.

6. Zhang, Y., Xu, W., Guo, H., Zhang, Y., He, Y., Lee, S.H., Song, X., Li, X., Guo, Y., Zhao, Y., et al. (2017). NOTCH1 Signaling Regulates Self-Renewal and Platinum Chemoresistance of Cancer Stem-like Cells in Human Non-Small Cell Lung Cancer. Cancer Res. *77*, 3082–3091.

7. Kitamura, H., Okudela, K., Yazawa, T., Sato, H., and Shimoyamada, H. (2009). Cancer stem cell: implications in cancer biology and therapy with special reference to lung cancer. Lung Cancer *66*, 275–281.

8. Pardal, R., Clarke, M.F., and Morrison, S.J. (2003). Applying the principles of stem-cell biology to cancer. Nat. Rev. Cancer *3*, 895–902.

9. Bartel, D.P. (2004). MicroRNAs: genomics, biogenesis, mechanism, and function. Cell *116*, 281–297.

10. Korpal, M., Ell, B.J., Buffa, F.M., Ibrahim, T., Blanco, M.A., Celià-Terrassa, T., Mercatali, L., Khan, Z., Goodarzi, H., Hua, Y., et al. (2011). Direct targeting of Sec23a by miR-200s influences cancer cell secretome and promotes metastatic colonization. Nat. Med. *17*, 1101–1108.

11. Gregory, P.A., Bert, A.G., Paterson, E.L., Barry, S.C., Tsykin, A., Farshid, G., Vadas, M.A., Khew-Goodall, Y., and Goodall, G.J. (2008). The miR-200 family and miR-205 regulate epithelial to mesenchymal transition by targeting ZEB1 and SIP1. Nat. Cell Biol. *10*, 593–601.

12. Gregory, P.A., Bracken, C.P., Smith, E., Bert, A.G., Wright, J.A., Roslan, S., Morris, M., Wyatt, L., Farshid, G., Lim, Y.Y., et al. (2011). An autocrine TGF-beta/ZEB/miR-200 signaling network regulates establishment and maintenance of epithelial-mesenchymal transition. Mol. Biol. Cell *22*, 1686–1698.

13. Zhang, J., Luo, N., Luo, Y., Peng, Z., Zhang, T., and Li, S. (2012). microRNA-150 inhibits human CD133-positive liver cancer stem cells through negative regulation of the transcription factor c-Myb. Int. J. Oncol. *40*, 747–756.

14. Liu, D.Z., Zhang, H.Y., Long, X.L., Zou, S.L., Zhang, X.Y., Han, G.Y., and Cui, Z.G. (2015). MIR-150 promotes prostate cancer stem cell development via suppressing p27Kip1. Eur. Rev. Med. Pharmacol. Sci. *19*, 4344–4352.

15. Xu, D.D., Zhou, P.J., Wang, Y., Zhang, Y., Zhang, R., Zhang, L., Chen, S.H., Fu, W.Y., Ruan, B.B., Xu, H.P., et al. (2016). miR-150 Suppresses the Proliferation and Tumorigenicity of Leukemia Stem Cells by Targeting the Nanog Signaling Pathway. Front. Pharmacol. *7*, 439.

16. Sun, Y., Su, B., Zhang, P., Xie, H., Zheng, H., Xu, Y., Du, Q., Zeng, H., Zhou, X., Chen, C., and Gao, W. (2013). Expression of miR-150 and miR-3940-5p is reduced in non-small cell lung carcinoma and correlates with clinicopathological features. Oncol. Rep. *29*, 704–712.

17. Zhang, L., Lin, J., Ye, Y., Oba, T., Gentile, E., Lian, J., Wang, J., Zhao, Y., Gu, J., Wistuba, I.I., et al. (2018). Serum MicroRNA-150 Predicts Prognosis for Early-Stage Non-Small Cell Lung Cancer and Promotes Tumor Cell Proliferation by Targeting Tumor Suppressor Gene SRCIN1. Clin. Pharmacol. Ther. *103*, 1061–1073.

18. Malanchi, I., Santamaria-Martínez, A., Susanto, E., Peng, H., Lehr, H.A., Delaloye, J.F., and Huelsken, J. (2011). Interactions between cancer stem cells and their niche govern metastatic colonization. Nature *481*, 85–89.

19. Sun, F.F., Hu, Y.H., Xiong, L.P., Tu, X.Y., Zhao, J.H., Chen, S.S., Song, J., and Ye, X.Q. (2015). Enhanced expression of stem cell markers and drug resistance in sphere-forming non-small cell lung cancer cells. Int. J. Clin. Exp. Pathol. *8*, 6287–6300.

20. Lin, C.C., Chou, C.H., Howng, S.L., Hsu, C.Y., Hwang, C.C., Wang, C., Hsu, C.M., and Hong, Y.R. (2009). GSKIP, an inhibitor of GSK3beta, mediates the N-cadherin/beta-catenin pool in the differentiation of SH-SY5Y cells. J. Cell. Biochem. *108*, 1325–1336.

21. Jin, H., Luo, S., Wang, Y., Liu, C., Piao, Z., Xu, M., Guan, W., Li, Q., Zou, H., Tan, Q.Y., et al. (2017). miR-135b Stimulates Osteosarcoma Recurrence and Lung Metastasis via Notch and Wnt/β-Catenin Signaling. Mol. Ther. Nucleic Acids 8, 111–122.

22. Kaur, H., Ali, S.Z., Huey, L., Hütt-Cabezas, M., Taylor, I., Mao, X.G., Weingart, M., Chu, Q., Rodriguez, F.J., Eberhart, C.G., and Raabe, E.H. (2016). The transcriptional modulator HMGA2 promotes stemness and tumorigenicity in glioblastoma. Cancer Lett. 377, 55–64.

23. Singh, I., Mehta, A., Contreras, A., Boettger, T., Carraro, G., Wheeler, M., Cabrera-Fuentes, H.A., Bellusci, S., Seeger, W., Braun, T., and Barreto, G. (2014). Hmga2 is required for canonical WNT signaling during lung development. BMC Biol. 12, 21.

24. Le, N., Sund, M., and Vinci, A.; GEMS collaborating group of Pancreas 2000 (2016). Prognostic and predictive markers in pancreatic adenocarcinoma. Dig. Liver Dis. 48, 223–230.

25. Shapiro, M., Akiri, G., Chin, C., Wisnivesky, J.P., Beasley, M.B., Weiser, T.S., Swanson, S.J., and Aaronson, S.A. (2013). Wnt pathway activation predicts increased risk of tumor recurrence in patients with stage I nonsmall cell lung cancer. Ann. Surg. 257, 548–554.

26. Hontecillas-Prieto, L., García-Domínguez, D.J., García-Mejías, R., Ramírez-Villar, G.L., Sáez, C., and de Álava, E. (2017). HMGA2 overexpression predicts relapse susceptibility of blastemal Wilms tumor patients. Oncotarget 8, 115290–115303.

27. Gao, X., Dai, M., Li, Q., Wang, Z., Lu, Y., and Song, Z. (2017). HMGA2 regulates lung cancer proliferation and metastasis. Thorac. Cancer 8, 501–510.

28. Stewart, D.J. (2014). Wnt signaling pathway in non-small cell lung cancer. J. Natl. Cancer Inst. 106, djt356.

29. Tang, W., Xu, P., Wang, H., Niu, Z., Zhu, D., Lin, Q., Tang, L., and Ren, L. (2018). MicroRNA-150 suppresses triple-negative breast cancer metastasis through targeting HMGA2. OncoTargets Ther. 11, 2319–2332.

30. Chou, H.Y., Howng, S.L., Cheng, T.S., Hsiao, Y.L., Lieu, A.S., Loh, J.K., Hwang, S.L., Lin, C.C., Hsu, C.M., Wang, C., et al. (2006). GSKIP is homologous to the Axin GSK3beta interaction domain and functions as a negative regulator of GSK3beta. Biochemistry 45, 11379–11389.

31. Dema, A., Schröter, M.F., Perets, E., Skroblin, P., Moutty, M.C., Deàk, V.A., Birchmeier, W., and Klussmann, E. (2016). The A-Kinase Anchoring Protein (AKAP) Glycogen Synthase Kinase 3β Interaction Protein (GSKIP) Regulates β-Catenin through Its Interactions with Both Protein Kinase A (PKA) and GSK3β. J. Biol. Chem. 291, 19618–19630.

32. Zha, L., Wang, Z., Tang, W., Zhang, N., Liao, G., and Huang, Z. (2012). Genome-wide analysis of HMGA2 transcription factor binding sites by ChIP on chip in gastric carcinoma cells. Mol. Cell. Biochem. 364, 243–251.

33. Thuault, S., Tan, E.J., Peinado, H., Cano, A., Heldin, C.H., and Moustakas, A. (2008). HMGA2 and Smads co-regulate SNAIL1 expression during induction of epithelial-to-mesenchymal transition. J. Biol. Chem. 283, 33437–33446.

34. Zha, L., Zhang, J., Tang, W., Zhang, N., He, M., Guo, Y., and Wang, Z. (2013). HMGA2 elicits EMT by activating the Wnt/β-catenin pathway in gastric cancer. Dig. Dis. Sci. 58, 724–733.

35. Wang, R.T., Xu, M., Xu, C.X., Song, Z.G., and Jin, H. (2014). Decreased expression of miR216a contributes to non-small-cell lung cancer progression. Clin. Cancer Res. 20, 4705–4716.

36. Zhang, W.C., Shyh-Chang, N., Yang, H., Rai, A., Umashankar, S., Ma, S., Soh, B.S., Sun, L.L., Tai, B.C., Nga, M.E., et al. (2012). Glycine decarboxylase activity drives non-small cell lung cancer tumor-initiating cells and tumorigenesis. Cell 148, 259–272.

37. Levina, V., Marrangoni, A.M., DeMarco, R., Gorelik, E., and Lokshin, A.E. (2008). Drug-selected human lung cancer stem cells: cytokine network, tumorigenic and metastatic properties. PLoS ONE 3, e3077.

38. Xu, C.X., Jere, D., Jin, H., Chang, S.H., Chung, Y.S., Shin, J.Y., Kim, J.E., Park, S.J., Lee, Y.H., Chae, C.H., et al. (2008). Poly(ester amine)-mediated, aerosol-delivered Akt1 small interfering RNA suppresses lung tumorigenesis. Am. J. Respir. Crit. Care Med. 178, 60–73.

39. Nuovo, G.J. (2010). In situ detection of microRNAs in paraffin embedded, formalin fixed tissues and the co-localization of their putative targets. Methods 52, 307–315.

40. Heng, W.S., Gosens, R., and Kruyt, F.A.E. (2019). Lung cancer stem cells: origin, features, maintenance mechanisms and therapeutic targeting. Biochem. Pharmacol. 160, 121–133.

41. Othumpangat, S., Bryan, N.B., Beezhold, D.H., and Noti, J.D. (2017). Upregulation of miRNA-4776 in Influenza Virus Infected Bronchial Epithelial Cells Is Associated with Downregulation of NFKBIB and Increased Viral Survival. Viruses 9, E94.